Geomechanics and Engineering, *Vol. 24, No. 5 (2021) 471-478*
DOI: https://doi.org/10.12989/gae.2021.24.5.471

Experimental research on the effect of water-rock interaction in filling media of fault structure

Dong Faxu, Peng Zhang, Wenbin Sun*, Shaoliang Zhou and Lingjun Kong

State Key Laboratory of Mining Disaster Prevention and Control,
College of Energy and Mining Engineering, Shandong University of Science and Technology, Qingdao 266590, China

(Received December 9, 2019, Revised February 18, 2021, Accepted March 2, 2021)

Abstract. Water damage is one of the five disasters that affect the safety of coal mine production. The erosion of rocks by water is a very important link in the process of water inrush induced by fault activation. Through the observation and experiment of fault filling samples, according to the existing rock classification standards, fault sediments are divided into breccia, dynamic metamorphic schist and mudstone. Similar materials are developed with the characteristics of particle size distribution, cementation strength and water rationality, and then relevant tests and analyses are carried out. The experimental results show that the water-rock interaction mainly reduces the compressive strength, mechanical strength, cohesion and friction Angle of similar materials, and cracks or deformations are easy to occur under uniaxial load, which may be an important process of water inrush induced by fault activation. Mechanical experiment of similar material specimen can not only save time and cost of large scale experiment, but also master the direction and method of the experiment. The research provides a new idea for the failure process of rock structure in fault activation water inrush.

Keywords: underground engineering; rock engineering; fault structure; filling media; similar materials; water-rock interaction; mechanical properties

1. Introduction

Fault structure is a high hazard area in coal mines and other underground projects, and it is also a disaster concentration area. The fault structure is a geological structure in which the strata are fractured after being subjected to the in-situ stress exceeding its own strength. This structure is filled with broken rock, clay, and other impurities, and is of low strength and stability. Fault fracture zone is usually a good channel for confined water to the working face, which may cause water inrush disaster from aquifer to working face (Das *et al*. 2018). Fault structure filling media refers to a kind of rock mass structure with specific fabric and relatively fragmented filling in the fault zone of the hangingwall and footwall of the fault (Scott and Mao 1993, Ngô and Natowitz 2016, Liu *et al*. 2018, Wu *et al*. 2019). Besides, the fault structure exists in the form of a weak zone, which is significantly different from the rock mass on both sides in the physical and mechanical properties. The filling media soaked in confined water is weakened by water and the mechanical properties are changed, thus affecting the stability and water conductivity of the whole fault structure. Therefore, it is of great significance to study the mechanism of fault activation instability and water inrush disaster to experiments on mechanical properties of filling media for water-induced rock mass weakening (Zhang *et al*. 2019, Feng *et al*. 2019, Quevedo and Bernaud 2018).

Wu *et al*. (2003) conducted a systematic experimental analysis and research on the deformation and failure modes of fault zone materials under different water content, different confining pressure and different loading modes through experiments such as indoor compression and creep. Wu and Liu (2003) used in-situ testing to test and evaluate the water-resisting capacity of filling media. It was concluded that the water-resisting capacity of rock mass in fault zone is generally 1/10-1/3 of that of intact rock mass.

In view of the above problems, by analyzing the water-rock interaction mechanism, considering the characteristics of fracture structure filling medium's disintegration resistance, cementation strength, and particle size distribution, the filling medium is divided into breccia, dynamic metamorphic schist and mudstone. And made the similar materials of filling media in fault structure based on the physical properties of the original rock to carry out the mechanical properties test of three filling media under water-rock interaction.

2. The mechanism of water-rock interaction

The Weakening Mechanism of underground confined water on filling media can be divided into physical weakening and chemical weakening. The physical weakening effect of underground confined water on filling media is mainly reflected in lubrication and softening. The chemical weakening effect of confined water on the filling

*Corresponding author, Associate Professor
E-mail: swb@sdust.edu.cn

ISSN: 2005-307X (Print), 2092-6219 (Online)

(a)Breccia (b)Dynamic metamorphic schist (c)Mudstone

Fig. 1 Schematic diagram of particle composition of fault structure filling media

medium of fault structure is mainly chemical erosion.

From the microscopic point of view, the water wedge interaction occurs between the filling particles and water molecules after the underground confined water intrudes into the fracture space. Water wedge action means that water molecules on the surface of filling particles tend to invade the space between particles due to adhesive force. When the compressive stress between the particles is not enough to resist the adhesion of water molecules, the water molecules will invade the gaps between the particles, causing the particle spacing to increase. On the macro structure, the cementation ability of the filling medium is weakened, which leads to the decrease of the shear strength and the friction between the filling medium and the hanging wall and foot wall. Finally, the slip structure of the fault structure is unstable and the water inrush channel is formed (Uyar and Babayigit 2016, Aksoy *et al*. 2016, Khoshnoudian *et al*. 2014).

At the same time, chemical erosion is carried out by ion exchange and dissolution. The ions in the water will replace the exchangeable ions in the medium, or react with the medium molecules when confined water flows through the fault filling medium. Finally, the structure and properties of the medium are changed, and the mechanical properties are also affected.

3. Classification of fault structure filling media and development of similar materials

3.1 Classification of filling media in fault structure

The fault-constructing water-induced disaster process is essentially the process of seepage and destruction of the fault structure filling media. Referring to relevant data and experiments, it is proposed that the disintegration resistance, cementation strength, particle gradation and the permeability of the transition surface of the filling media in contact with the upper and lower plates of the fault media are the main factors affecting the permeability characteristics of the filling media. Based on this, the filling media is divided into the following three types (GB/T 17412.2-1998):

The breccia filling media is mostly present in the tensile faults at the surface of 1-4 km. The structure of the media rock is loose and the integrity is poor. The composition of the media consists of a single particle with a sharp-edged shape, the particle size is generally greater than 2 mm, and the particles are filled with fine particles. The breccia filling media is prone to softening deformation when exposed to water, poor disintegration resistance, general cementation strength, and weak compaction state. The media and the structure are rough in contact with each other, the bonding force is low, and the layering changes obviously. The particle characteristics of breccia filling medium are shown in Fig. 1(a).

Dynamic metamorphic schist filling media are mostly found in the fractures with dynamic properties of compression and shear, such as the reverse fault formed by horizontal compression and gravity. Most of the rock masses that make up the media are compressed schist, which are dense and intact, and usually exist in a regional continuous state. The Dynamic metamorphic schist fault structure filling media has a small degree of water softening deformation, good anti-disintegration effect, high cementation strength, and small particle size, generally between 0.25-0.5 mm. The media is full and compact, and the compacted state is good, and it is closely adhered to the two plates of the structure, and the rock bedding continuity is strong. From the overall analysis, the Dynamic metamorphic schist filling media has low permeability and high compressive strength. The composition characteristics of the dynamic flaky rock filling media are shown in Fig. 1(b). The media is full and compact, and the compacted state is good, and it is closely adhered to the two plates of the structure, and the rock bedding continuity is strong. From the overall analysis, the Dynamic metamorphic schist filling media has low permeability and high compressive strength. The composition characteristics of the Dynamic metamorphic schist filling media are shown in Fig. 1(b).

The mudstone filling media is mainly developed in the shallow brittle fracture of the crust. The surface water carries a large amount of mud into the tectonic fracture, and the original fine gravel particles in the fault structure are mixed and glued to form a muddy rock formation. The rock formation is weakly consolidated. The compressive strength is lower than most rock masses. The main component of the mudstone filling media is clay, and the cementation effect is

general. The bonding strength between the media and the fractured plate is weak, and the friction is small. When a strong hydraulic erosion is encountered, the contact surface is easy to form a water guiding channel. On the whole, the media has a high clay content and good water blocking effect, but the compressive strength is low. The particle composition characteristics of argillaceous filling media are shown in Fig. 1(c).

3.2 Development of similar materials for fracture structure filling media

In this paper, we developed similar materials for the fracture structure filling media based on the experimental methods of laboratory experiments and the characteristics of the original rock of the filling media (Li *et al*. 2010, Yin *et al*. 2018, Zhang *et al*. 2019). The angular coarse sand and fine sand are used as the aggregate, the coarse sand has a particle size of 2-5 mm, and the fine sand has a particle size of 0.25-1 mm. Calcium carbonate simulates the fine particles among the large particles in the filling medium, which enables the coarse sand to gather in the material and form some clumps composed of several coarse sand particles. The coarse sand particles form micro-agglomerates; cement and vaseline are cementing agents, in which cement is a brittle cement, cement reacts with water to simulate the dielectric siliceous cement, vaseline is a plastic binder, and cement and vaseline work together to make the material meet the performance requirements in strength and disintegration; hydraulic oil acts as a conditioning agent for the material's water rationality, reconciling the permeability of similar materials.

Comprehensive analysis of the basic characteristics of the three kinds of filling media, this paper uses angular grit, calcium carbonate, cement, Vaseline , hydraulic oil to develop similar materials for breccia filling media, hereinafter set as C material; A similar material using a fine sand, calcium carbonate, cement, Vaseline , hydraulic oil to develop a dynamic metamorphic schist filling media, hereinafter set as F material; A similar material for the mudstone filling media is prepared by using clay, calcium carbonate, Vaseline and hydraulic oil, and is hereinafter set as the S material. In order to facilitate the experiment, the simulated materials are made into standard specimens by means of dies. The standard specimen is a cylinder with a diameter of 50 mm and a height of 100 mm.

In this paper, the single-factor experimental method is used to compare the similar materials. Through a large number of matching experiments, the matching schemes of three basic filling materials are determined. The matching schemes are shown in Tables 3.1-3.3.

Table 3.1 Ratio table of similar materials in breccia

Project number	Material Ratio (Coarse Sand, Calcium Carbonate, Cement, Vaseline, Hydraulic Oil)	Specimen number
C1	10 : 1.5 : 0.8 : 0.8 : 0.4	C11 ~ C18
C2	10 : 1.5 : 1.0 : 0.6 : 0.4	C21 ~ C28
C3	10 : 2.0 : 1.0 : 0.4 : 0.5	C31 ~ C38
C4	10 : 2.5 : 0.8 : 0.4 : 0.6	C41 ~ C48

Table 3.2 Ratio table of similar materials in dynamic metamorphic schist

Project number	Material Ratio (Fine Sand, Calcium Carbonate, Cement, Vaseline, Hydraulic Oil)	Specimen number
F1	10 : 1.5 : 0.6 : 0.4 : 0.4	F11 ~ F18
F2	10 : 1.5 : 0.8 : 0.8 : 0.4	F21 ~ F28
F3	10 : 2.0 : 0.6 : 0.8 : 0.5	F31 ~ F38
F4	10 : 2.5 : 0.8 : 0.4 : 0.6	F41 ~ F48

Table 3.3 Ratio table of similar materials in Mudstone

Project number	Material Ratio (Clay, Calcium Carbonate, Vaseline, Hydraulic Oil)	Specimen number
S1	4 : 1.0 : 0.4 : 0.4	S11 ~ S18
S2	4 : 1.5 : 0.6 : 0.3	S21 ~ S28
S3	4 : 0.7 : 0.2 : 0.5	S31 ~ S38
S4	4 : 0.7 : 0.6 : 0.5	S41 ~ S48

Fig. 2 The composition of similar materials

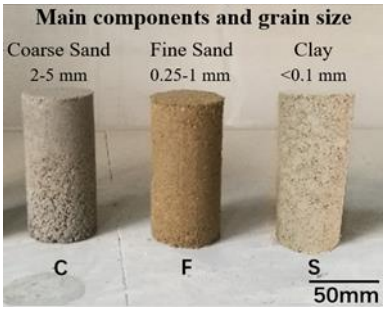

Fig. 3 Comparison of specimen forming

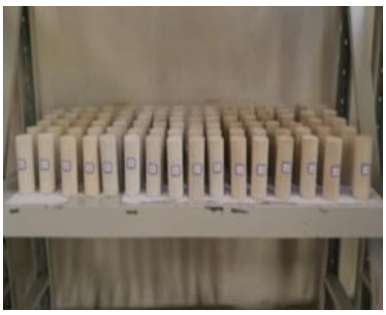

Fig. 4 Sample maintenance

• According to the properties of material components, the configuration process can be divided into the following steps:

• Weigh aggregate, filling agent and cementitious agent

Fig. 5 Shimadzu AG-X250 electronic universal testing machine

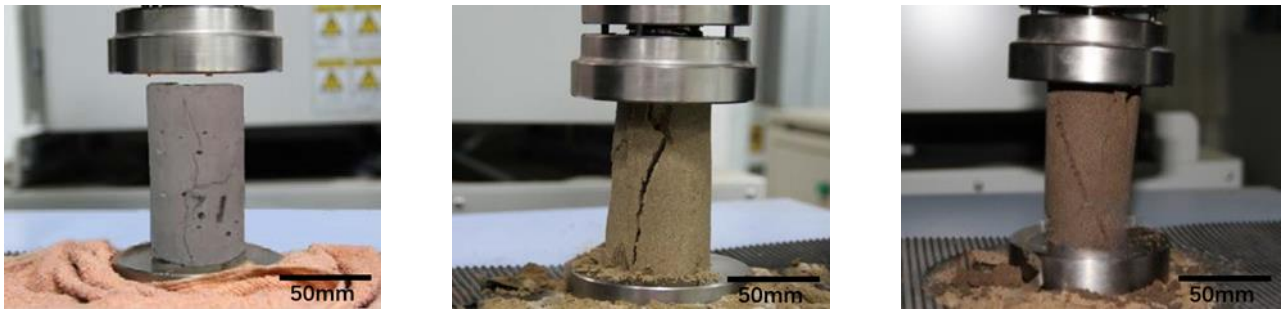

Fig. 6 Some specimens of uniaxial load test

according to the set proportion and weight in the experimental design scheme.

• Place the weighed aggregate, filling agent and cementing agent in a smooth waterproof mixing basin and mix evenly.

• Pour the hydraulic oil and water into the mixing basin in turn to mix well with the material.

• Heat the Vaseline was to 45-50°C to make it liquefied and mixed with the material quickly and fully.

• Load the stirred analogue material quickly into the double-opening die, and make the material cemented and solidified under uniform force.

• Stay for 20 minutes, choose the machine for demoulding treatment, place at room temperature maintenance.

• Number the similar material model to be inspected after 24 hours.

Fig. 2 shows the composition of similar materials. Figure 3 shows the comparison of specimen forming. Fig. 4 shows the sample maintenance.

4. Experimental study on influence of water-rock interaction of fracture structure filling media

Fault structure is an important way to communicate groundwater. The fault structure filling media is often in the water environment. The filling media is weakened by groundwater. The weakening effect of the media from solid to plastic or even liquid is enhanced. The fault structure filling media softens and mud The phenomenon of cohesion and friction angle of the media body is greatly reduced, the mechanical properties are changed, and the activation instability and catastrophe are induced (Moosa and Seyed 2018, Schopfer *et al*. 2016).

4.1 Purpose of the experiment

Aiming at the weakening effect of the fault structure filling media in the water environment, the experimental study on the mechanical properties of the fault structure filling water and rock weakening is carried out, and the influencing factors of the induced fault activation instability are revealed. Foundation of the disaster mechanism research.

4.2 Experimental plan

The standard test piece of similar material φ50 mm×100 mm was developed as the experimental object. The stress and strain characteristic values obtained by uniaxial compression test were carried out under the conditions of non-immersion test and 48 hours of water immersion in the standard test piece after air-drying. Characterization parameters of the influence of water-rock weakening effect on the mechanical properties of filling media.

In this section, two sets of comparative experiments are designed. In the first set of experiments, the test pieces after air-drying are directly subjected to uniaxial compression test; in the second set of experiments, the test pieces after air-drying are placed in water for 48 hours, and then Uniaxial compression experiments. Two similar materials, C and F, each of which was tested in the first group and the second group under the same ratio. Since the S material was soaked in water for 48 hours, the softening and swelling

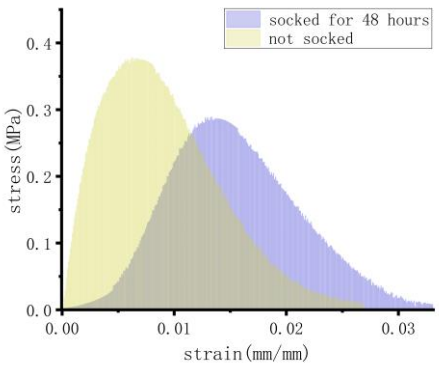

(a)C1

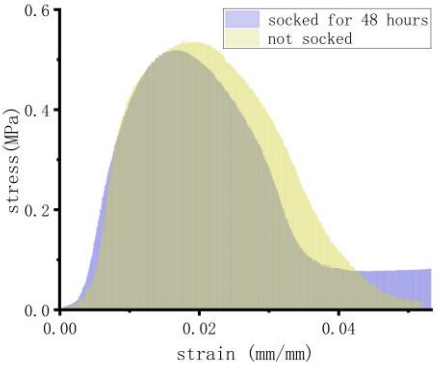

(b)C2

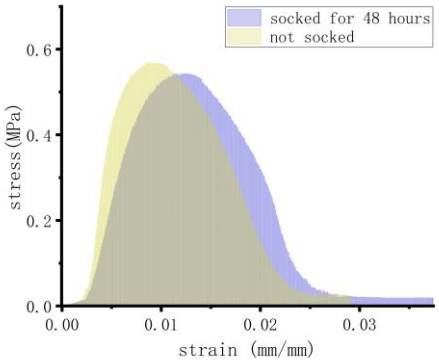

(c)C3

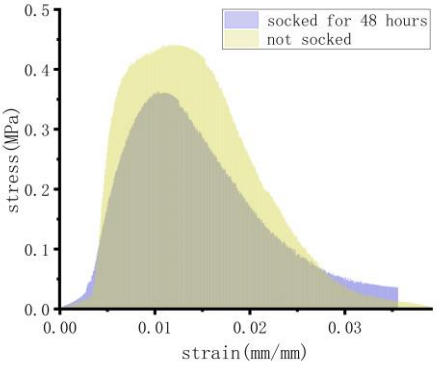

(d)C4

Fig. 7 Full stress and strain curve of C specimen pre and post water immersion

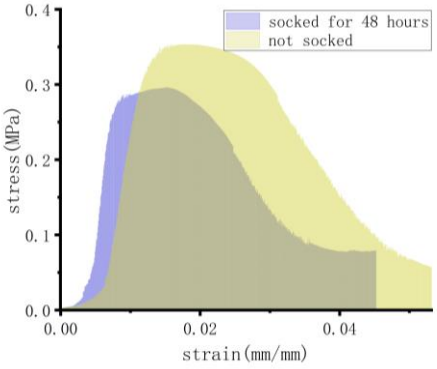

(a)F1

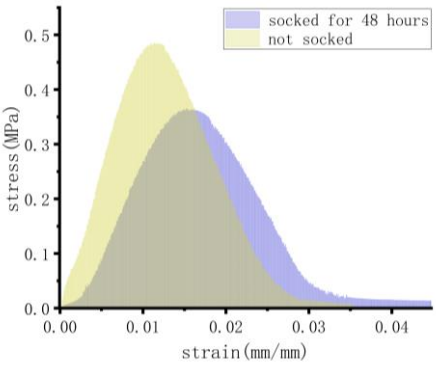

(b)F2

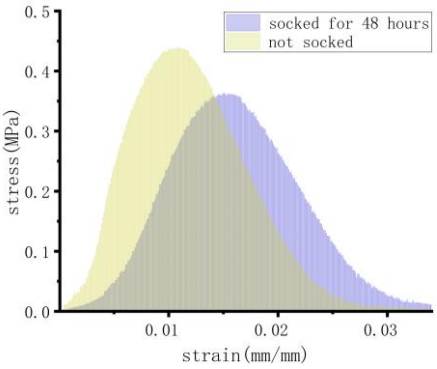

(c)F3

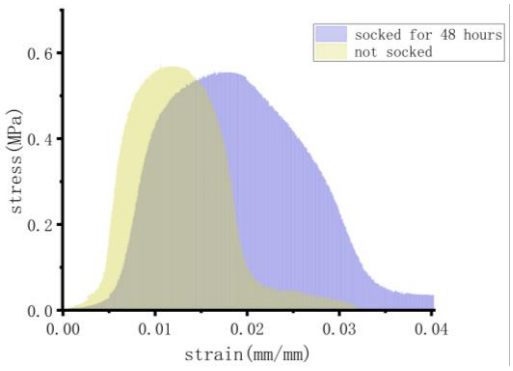

(d)F4

Fig. 8 Full stress and strain curve of F specimen pre and post water immersion

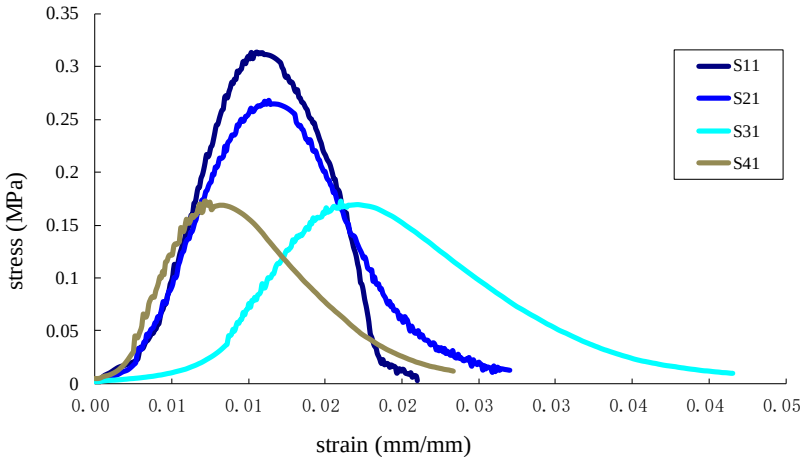

Fig. 9 Full stress and strain curve of S specimen pre and post water immersion

degree was high, and the semi-solid soft mud was formed, and the uniaxial compression experiment after the water immersion could not be performed. Therefore, the S material was only subjected to the first group experiment. Uniaxial compression experiments were performed on a Shimadzu AG-X250 electronic universal testing machine, as shown in Fig. 5.

4.3 Experimental result

The uniaxial compression data provided by the Shimadzu AG-X250 electronic universal testing machine was collected and the full stress-strain curves of the material samples under the same ratio were obtained under the conditions of not being soaked in water and soaked for 48 hours.

Fig. 7 shows the comparison of the full stress-strain curves of the C material obtained before and after immersion. Fig. 7(a)-7(d) represent the four ratios of the C materials C1 to C4, respectively. As shown in the figure, in the two sets of experiments, the compressive strength and peak strain test results of the specimens under the same ratio are different. Combined with the graphs (a) to (d), the general law can be found, and the specimens are pressed in the first group of experiments. The compressive strength of the specimen before immersion is greater than that after immersion, and the peak strain in the test before immersion is smaller than that in the experiment after immersion.

Fig. 8 shows the comparison of the full stress-strain curves of the F material obtained in the experiment before and after immersion, and Fig. 8(a)-8(d) represent the four ratios of the F materials F1 to F4, respectively. Combined with the curve, it can be found that the compressive strength and peak strain of material F are similar to that of material C in numerical value and overall law. The compressive strength of material F in the pre immersion test is greater than that in the post immersion test, and the peak strain in the pre immersion test is smaller than that in the post immersion test.

Fig. 9 is a graph showing the uniaxial compression full stress-strain curve of the S material specimen after drying in the state of not soaking. As shown in the figure, the stress-strain curves of the specimens under different ratios are different. The change of other components such as calcium carbonate, petrolatum and hydraulic oil will change the compressive strength and peak strain when the content is the same, which indicates that the comprehensive performance of the material can be controlled by controlling the distribution ratio of the materials.

4.4 Analysis of experimental results

From the normal stress-strain curve rule before and after the water immersion of the test piece in Fig. 7 and 8, in the experiment before immersion, the stress increases rapidly as the strain increases, and when the stress reaches the peak intensity, the stress value suddenly decreases. This form of failure exhibits a significant brittle failure characteristic, which has no obvious yielding phenomenon, a high value of the failure strength, and a small strain value at the time of failure, that is, the stress reaches a maximum value under a small strain.

In the experiment after immersion in water, the pressurized test piece was in a saturated state, and the stress-strain curve at the initial stage of compression was more curved than that of the first set of experiments. This was due to the softening of the test piece after 24 hours of water immersion. The water expands or the surface material of the test piece appears slightly loose, and the bending phase of the curve is actually the stage of compaction deformation experienced by the test piece. After the compaction deformation stage, the stress increases with the increase of the strain. It can be seen from the curve that the stress growth rate is generally lower than that of the first group of experiments. As the stress reaches the yield strength, the strain growth rate increases, the stress growth rate decreases, and the stress-strain relationship shows a significantly convex curve. When the stress reaches the peak strength, the test piece breaks, the material strain growth rate further increases, and the compressive strength value continues to decrease (Kristensen *et al*. 2016, Valoroso *et al*. 2014).

The stress-strain curves of the specimens before and after immersion were compared and analyzed. It was concluded that after the material was soaked in water, a significant softening effect appeared, which showed that the

Table 4 Uniaxial compressive strength and modulus of partial specimen

Specimen number (No water immerse)	Rc/MPa	E/MPa	Specimen number (Soaked for 48 hours)	Rc/MPa	E/MPa
C11	0.38	53.24	C12	0.29	21.79
C21	0.54	79.97	C22	0.52	49.51
C31	0.57	83.89	C32	0.53	57.70
C41	0.43	46.30	C42	0.36	26.41
F11	0.35	37.62	F12	0.30	19.85
F21	0.48	96.74	F22	0.36	71.36
F31	0.44	53.13	F32	0.37	44.17
F41	0.57	75.49	F42	0.56	57.15
S11	0.28	31.43			
S21	0.20	23.27			
S31	0.25	19.87			
S41	0.16	10.65			

required stress value was lower when the specimen was damaged, but the shape was The variables are larger. This explains the weakening effect of water rock, which can reduce the compressive strength of rock mass and increase the compressive deformation of rock mass, so that the rock mass is more likely to break the crack under the influence of stress disturbance and affect the water conductivity and stability of the fault structure.

The compressive strength and elastic modulus of specimens before and after immersion are calculated and counted. The statistical results are shown in Table 4.

As shown in Table 4, the average compressive strength of the C material was 0.42 MPa, and the average elastic modulus was 51.18 MPa; the average compressive strength after immersion for 48 hours was 0.35 MPa, and the average elastic modulus was 29.92 MPa. The average compressive strength of the F material samples was 0.53Mpa, the average elastic modulus was 89.45Mpa; the average compressive strength after immersion for 48 hours was 0.45Mpa, and the average elastic modulus was 63.13Mpa. The average compressive strength of each sample of the S material was 0.22 MPa, and the average elastic modulus was 21.31 MPa. The average compressive strength and elastic modulus of three similar materials of S, C and F are: S material <C material <F material. For both C and F materials, the compressive strength and elastic modulus were reduced after 48 hours of water immersion.

5. Conclusions

This paper studies the water-rock interaction of similar materials in the fault filling medium, laying a foundation for large-scale simulation experiments of similar materials to the fault filling material, and providing ideas for studying the formation of water inrush channels in the fault filling medium. The following results have been achieved in this experiment:

• According to the existing rock classification standards, the fault sediments were divided into three types: breccia, dynamic metamorphic schist and argillite. After observation and experiments on the samples of fault fillers, the fault sediments were classified into breccia, dynamic metamorphic schist and mudstone according to the existing rock classification standards. Similar materials are developed with the characteristics of particle size distribution, cementation strength and water rationality, and then relevant tests and analyses are carried out.

• The weakening effect of water on the filling medium is related to the characteristics of the medium. The results show that the dynamic metamorphic schist in filling medium has dense structure, high cementation strength, low weakening degree and high compressive strength after immersion. Breccia filling medium has low strength, easy to form connected pores and good permeability. After immersion, the degree of weakening is large and compressive strength is general. The compressive strength of mudstone is the lowest, and the structure is easy to be damaged after immersion. The weakening effect of confined water on the filling medium of fault structure is mainly manifested in the reduction of compressive strength and enhancement of plasticity of filling medium. After the filling medium is weakened, it is easy to produce cracks or deformation under compression, the mechanical strength decreases, the cohesion and friction angle decrease. This may be an important process of water inrush from fault activation.

• Mechanical experiment of similar material specimen can not only save time and cost of large scale experiment, but also master the direction and method of the experiment. We confirmed the experimental method of large-scale similar materials through the experiments of similar materials filled with medium. It can be predicted that breccia will provide a good water conducting path in the fault structure constructed by fault fillings with similar materials, and the instability of fault structure will start from the softening deformation of mudstone. The filling material in the pressure concentration area is more likely to cause structural failure under the influence of water in the actual fault. The research provides a new idea for the failure process of rock structure in fault activation water inrush.

Acknowledgments

This research was financially supported by the National Natural Science Foundation of China (51974172), Natural Science Foundation of Shandong Province (ZR2019MEE004), Innovation and Technology Program of universities in Shandong Province, China (2020KJH001), Supported by China Postdoctoral Science Foundation (2020T130386), Elite program of Shandong University of science and technology.

References

Aksoy, C.O., Uyar, G.G. and Ozcelik, Y. (2016), "Comparison of Hoek-Brown and Mohr-Coulomb failure criterion for deep open coal mine slope stability", *Struct. Eng. Mech.*, **60**(5), 809-828.

https://doi.org/10.12989/sem.2016.60.5.809.
Das A.J., Mandal P.K., Sahu S.P., Kushwaha A., Bhattacharjee R. and Tewari S. (2018), "Evaluation of the effect of fault on the stability of underground workings of coal mine through DEM and statistical analysis", *J. Geol. Soc. India*, **92**(6), 732-742. https://doi.org/10.1007/s12594-018-1096-2.
Feng, F., Chen, S.J., Li, D.Y., Hu, S.T., Huang, W.P. and Li, B. (2019), "Analysis of fractures of a hard rock specimen via unloading of central hole with different sectional shapes", *Energy Sci. Eng.*, **7**(6), 2265-2286. https://doi.org/10.1002/ESE3.432.
GB/T 17412.2-1998 (1998), Classification and namenclature schemes of the rocks, State Administration for Market Regulation, China.
Khoshnoudian, F., Ahmadi, E., Sohrabi, S. and Kiani, M. (2014), "Higher-mode effects for soil-structure systems under different components of near-fault ground motions", *Earthq. Struct.*, **7**(1), 83-99. https://doi.org/10.12989/eas.2014.7.1.083.
Kristensen, T.B., Rotevatn, A., Peacock, D.C., Henstra, G.A., Midtkandal, I. and Grundvåg, S.A. (2016), "Structure and flow properties of syn-rift border faults: The interplay between fault damage and fault-related chemical alteration (Dombjerg Fault, Wollaston Forland, NE Greenland)", *J. Struct. Geol.*, **92**, 99-115. https://doi.org/10.1016/j.jsg.2016.09.012.
Li, S., Feng, X., Li, L. and Li, G. (2010), "Research and development of a new similar material for solid-fluid coupling and its application", *Chin. J. Rock Mech. Eng.*, **29**(2), 281-288.
Liu, F., Guo, Z., Lv, H. and Cheng, Z. (2018), "Test and analysis of blast wave in mortar test block", *Int. J. Rock Mech. Min. Sci.*, **108**, 80-85. https://doi.org/10.1016/j.ijrmms.2018.06.003.
Mazloom, M., Homayooni, S.M. and Miri, S.M. (2018), "Effect of rock flour type on rheology and strength of self-compacting lightweight concrete", *Comput. Concrete*, **21**(2), 199-207. https://doi.org/10.12989/cac.2018.21.2.199.
Ngô, C. and Natowitz, J.B. (2016), *Coal* in *Our Energy Future*, John Wiley & Sons, Inc. Hoboken, New Jersey, U.S.A.
Quevedo, F.P. Bernaud, D. (2018), "Parametric study of the convergence of deep tunnels with long term effects, Abacuses", *Geomech. Eng.*, **15**(4), 973-986. https://doi.org/10.12989/gae.2018.15.4.973.
Schöpfer, M.P., Childs, C., Walsh, J.J. and Manzocchi, T. (2016), "Evolution of the internal structure of fault zones in three-dimensional numerical models of normal faults", *Tectonophysics*, **666**, 158-163. https://doi.org/10.1016/j.tecto.2015.11.003.
Scottt, A.C. and Mao, B.Z. (1993), "The coal geology of China" *Geology Today*, **9**(1), 14-18. https://doi.org/10.1111/j.1365-2451.1993.tb00969.x.
Uyar, G.G. and Babayigit, E. (2016), "Guided wave formation in coal mines and associated effects to buildings", *Struct. Eng. Mech.*, **60**(6), 923-937. https://doi.org/10.12989/sem.2016.60.6.923.
Valoroso, L., Chiaraluce, L. and Collettini, C. (2014), "Earthquakes and fault zone structure", *Geology*, **42**(4), 343 346. https://doi.org/10.1130/G35071.1.
Wu, J.W. and Liu, X.H. (2003), "In-situ measurement study and evaluation on water-resisting ability of rock mass in fault zone", *Rock Soil Mech.*, **24**(10),k 447-450. https://doi.org/10.16285/j.rsm.2003.s2.106.
Wu, Q., Zhou, Y.J., Liu, J.T., Zhong, Y.P., Li, J.M. and Zhou, R.G. (2003), "The mechanical experiment study on lag mechanism of water-bursting of fault under coal seam", *J. China Coal Soc.*, **28**(6), 561-565. https://doi.org/10.1007/s11769-003-0003-x.
Wu, X., Jiang, Y., Wang, G., Gong, B., Guan, Z. and Deng, T. (2019), "Performance of a new yielding rock bolt under pull and shear loading conditions", *Rock Mech. Rock Eng.*, **52**(9), 3401-3412. https://doi.org/10.1007/s00603-019-01779-8.
Yin, D.W., Chen, S.J., Liu, X.Q. and Ma, H.F. (2018), "Effect of joint angle in coal on failure mechanical behavior of roof rock-coal combined body", *Q. J. Eng. Geol. Hydroge.*, **51**, 202-209. https://doi.org/10.1144/qjegh2017-041.
Zhang, G.C., Wen, Z.J., Liang, S.J., Tan, Y.L., Tian, L., Zhao, Y.Q. and Zhao, D. S. (2019), "Ground response of a gob-side entry in a longwall panel extracting 17m-thick coal seam: A case study", *Rock Mech. Rock Eng.*, **53**(2), 497-516. https://doi.org/10.1007/s00603-019-01922-5.
Zhang, Y., Cheng, Z. and Lv, H. (2019), "Study on failure and subsidence law of frozen soil layer in coal mine influenced by physical conditions", *Geomech. Eng.*, **18**(1), 97-109. https://doi.org/10.12989/gae.2019.18.1.97

CC